AFRL-RZ-WP-TP-2012-0151

THE EFFECT OF STRAIN ON GRAINS AND GRAIN BOUNDARIES IN $YBa_2Cu_3O_{7-\delta}$ COATED CONDUCTORS (POSTPRINT)

D.C. van der Laan

University of Colorado

T.J. Haugan and P.N. Barnes

Mechanical Energy Conversion Branch
Energy/Power/Thermal Division

D. Abraimov, F. Kametani, and D.C. Larbalestier

Florida State University

M.W. Rupich

American Superconductor Corporation

FEBRUARY 2012

AIR FORCE RESEARCH LABORATORY
PROPULSION DIRECTORATE
WRIGHT-PATTERSON AIR FORCE BASE, OH 45433-7251
AIR FORCE MATERIEL COMMAND
UNITED STATES AIR FORCE

REPORT DOCUMENTATION PAGE

Form Approved
OMB No. 0704-0188

1. REPORT DATE *(DD-MM-YY)*	2. REPORT TYPE	3. DATES COVERED *(From - To)*
February 2012	Journal Article Postprint	03 May 2008 – 03 May 2010

4. TITLE AND SUBTITLE

THE EFFECT OF STRAIN ON GRAINS AND GRAIN BOUNDARIES IN $YBa_2Cu_3O_{7-\delta}$ COATED CONDUCTORS (POSTPRINT)

5a. CONTRACT NUMBER
In-house

5b. GRANT NUMBER

5c. PROGRAM ELEMENT NUMBER
62203F

6. AUTHOR(S)

D.C. van der Laan (University of Colorado)
T.J. Haugan and P.N. Barnes (AFRL/RZPG)
D. Abraimov, F. Kametani, and D.C. Larbalestier (Florida State University)
M.W. Rupich (American Superconductor Corporation)

5d. PROJECT NUMBER
3145

5e. TASK NUMBER
32

5f. WORK UNIT NUMBER
314532ZE

7. PERFORMING ORGANIZATION NAME(S) AND ADDRESS(ES)

University of Colorado
Department of Physics
Boulder, CO 80309

Florida State University
National High Magnetic Field Laboratory
Tallahassee, FL 32310

Mechanical Energy Conversion Branch (AFRL/RZPG)
Energy/Power/Thermal Division
Air Force Research Laboratory, Propulsion Directorate
Wright-Patterson Air Force Base, OH 45433-7251
Air Force Materiel Command, United States Air Force

American Superconductor Corporation
Westborough, MA 01598

8. PERFORMING ORGANIZATION REPORT NUMBER
AFRL-RZ-WP-TP-2012-0151

9. SPONSORING/MONITORING AGENCY NAME(S) AND ADDRESS(ES)

Air Force Research Laboratory
Propulsion Directorate
Wright-Patterson Air Force Base, OH 45433-7251
Air Force Materiel Command
United States Air Force

10. SPONSORING/MONITORING AGENCY ACRONYM(S)
AFRL/RZPG

11. SPONSORING/MONITORING AGENCY REPORT NUMBER(S)
AFRL-RZ-WP-TP-2012-0151

12. DISTRIBUTION/AVAILABILITY STATEMENT

Approved for public release; distribution unlimited.

13. SUPPLEMENTARY NOTES

Journal article published in *Superconductor Science and Technology*, Vol. 23, 2010. This paper contains color.

 PA Case Number: 88ABW-2009-2133; Clearance Date: 03 May 2010.

14. ABSTRACT

The role of grains and grain boundaries in producing reversible strain effects on the transport current critical current density (J_c) of $YBa_2Cu_3O_{7-\delta}$ (YBCO) coated conductors that are produced with metal–organic deposition (MOD) was investigated. The strain (ε) dependence of J_c for full-width coated conductors is compared with that for samples in which the current transport was limited to a few or single grain boundaries by cutting narrow tracks with a laser or focused ion beam, as well as with thin films deposited on bicrystalline $SrTiO_3$ substrates by use of pulsed-laser deposition (PLD). Our results show that the dependences of J_c on ε for the grains and for the grain boundaries from the two kinds of YBCO samples can be expressed by the same function, however with a greater effective tensile strain at the grain boundaries than in the grains. The really striking result is that the grain boundary strain is 5–10 times higher for grain boundaries of in situ PLD grown bicrystals as compared to the aperiodic, meandered, nonplanar grain boundaries that develop in ex situ grown MOD-YBCO in the coated conductor of this study.

15. SUBJECT TERMS

grains, boundaries, strain, organic, laser, coated, pulsed, conductor, nonplanar, function, beam, ion, transport, density, current

16. SECURITY CLASSIFICATION OF:			17. LIMITATION OF ABSTRACT:	18. NUMBER OF PAGES	19a. NAME OF RESPONSIBLE PERSON (Monitor)
a. REPORT	b. ABSTRACT	c. THIS PAGE			Timothy J. Haugan
Unclassified	Unclassified	Unclassified	SAR	14	19b. TELEPHONE NUMBER *(Include Area Code)* N/A

Supercond. Sci. Technol. **23** (2010) 014004 (7pp) doi:10.1088/0953-2048/23/1/014004

The effect of strain on grains and grain boundaries in $YBa_2Cu_3O_{7-\delta}$ coated conductors*

D C van der Laan[1,2], T J Haugan[3], P N Barnes[3], D Abraimov[4], F Kametani[4], D C Larbalestier[4] and M W Rupich[5]

[1] Department of Physics, University of Colorado, Boulder, CO 80309, USA
[2] National Institute of Standards and Technology, Boulder, CO 80305, USA
[3] Air Force Research Laboratory, Wright-Patterson AFB, OH 45433, USA
[4] National High Magnetic Field Laboratory, Florida State University, Tallahassee, FL 32310, USA
[5] American Superconductor Corporation, Westborough, MA 01598, USA

E-mail: danko@boulder.nist.gov

Received 1 August 2009, in final form 13 August 2009
Published 9 December 2009
Online at stacks.iop.org/SUST/23/014004

Abstract

The role of grains and grain boundaries in producing reversible strain effects on the transport current critical current density (J_c) of $YBa_2Cu_3O_{7-\delta}$ (YBCO) coated conductors that are produced with metal–organic deposition (MOD) was investigated. The strain (ε) dependence of J_c for full-width coated conductors is compared with that for samples in which the current transport was limited to a few or single grain boundaries by cutting narrow tracks with a laser or focused ion beam, as well as with thin films deposited on bicrystalline $SrTiO_3$ substrates by use of pulsed-laser deposition (PLD). Our results show that the dependences of J_c on ε for the grains and for the grain boundaries from the two kinds of YBCO samples can be expressed by the same function, however with a greater effective tensile strain at the grain boundaries than in the grains. The really striking result is that the grain boundary strain is 5–10 times higher for grain boundaries of *in situ* PLD grown bicrystals as compared to the aperiodic, meandered, nonplanar grain boundaries that develop in *ex situ* grown MOD-YBCO in the coated conductor of this study.

1. Introduction

Vast technical improvements in substrate processing and thin film deposition techniques have resulted in remarkable progress in high-temperature superconductor (HTS) development, with almost single-crystalline-like $YBa_2Cu_3O_{7-\delta}$ films on textured templates achieving critical current densities of 3–4 MA cm^{-2} over lengths exceeding 1000 m [1–3]. Current blocking by grain boundaries has been eliminated as much as possible in these conductors by reducing the misorientation angle θ at which grains are connected. Several mechanisms that limit the critical current density across grain boundaries have been identified [4–15], especially the important role of grain boundary dislocation cores that limit the superconducting channel cross-section at low angles ($<10°$).

The superconducting film in coated conductors is relatively brittle. Hence, for engineering purposes we need to measure the maximum axial strain that can be applied before the superconductor breaks (the irreversible strain limit ε_{irr}) [16–18]. The critical current density shows only a small reversible strain dependence in $Bi_2Sr_2Ca_2Cu_3O_x$ (Bi-2223) tapes below ε_{irr} [19, 20]; however, a much larger reversible change with strain below ε_{irr} is measured in $YBa_2Cu_3O_{7-\delta}$ coated conductors [21–23]. This reversible change in J_c is intrinsic to the superconductor and occurs before the material breaks. Especially under axial compressive strain, the reversible change in J_c for YBCO coated conductors is

* Work partially supported by NIST, a US government agency, not subject to US copyright. Certain commercial materials are referred to in this paper to foster understanding. Such identification does not imply recommendation or endorsement by NIST, nor does it imply that the materials identified are necessary the best available for the purpose.

significant. In this case, J_c decreases reversibly by 40% at −1% strain at 76 K in self-field [24]. This effect has major implications for applications where the conductor is subjected to high axial stresses, because J_c may be much lower during operation compared to that of the conductor's unstrained state. The effect of strain on J_c may even be enhanced by the application of a magnetic field, which has recently been demonstrated [25–27].

The origin of the reversible strain effect in YBCO coated conductors remains unknown. Because coated conductors are polycrystalline, whether the strain effect originates from within the YBCO grains or at the grain boundaries is unclear. Reversible changes in superconducting properties of the cuprates with stress or strain were observed long before coated conductors emerged. Pressure is known to produce a large change in critical temperature (T_c) of high-temperature superconductors, with the most prominent example being the increase in T_c of $HgBa_2Ca_2Cu_3O_{8+\delta}$ from 134 to 164 K under 31 GPa hydrostatic pressure [28]. The variation in distance between the apical oxygen and the CuO_2 planes with strain and the change in tetragonality with pressure are likely causes of the change in T_c [29–32]. Uniaxial pressure experiments on untwinned YBCO single crystals revealed that the change in T_c with pressure oriented along the a-axis (ε_a) is opposite to the change in T_c when strain is applied along the b-axis (ε_b): $dT_c/d\varepsilon_a = 230$ K, and $dT_c/d\varepsilon_b = -220$ K. The change is less pronounced when the lattice is strained along the c-axis ($dT_c/d\varepsilon_c = 18$ K) [32–34]. Strain also influences the chemical composition of the superconductor during its formation; for instance when deposited on substrates with lattice constants that are slightly different from those of the superconducting film [35–38]. Also, Chisholm and Pennycook claimed that strain fields around grain boundary (GB) dislocations exceeding approximately 1% prevent the transformation from a nonsuperconducting tetragonal structure to a superconducting orthorhombic structure during grain boundary formation [5].

It has recently been shown that applied compressive strain strongly enhances the J_c at [001]-tilt grain boundaries in YBCO films that were deposited on bicrystalline $SrTiO_3$ (STO) substrates [39]. The strain dependence of J_c of both single-crystalline and bicrystalline films grown on STO were described by the same power-law function, the principal difference between the two types of films being the initial strain state of the YBCO; grain boundaries are under a much larger axial tensile strain compared to that of the grains (in some cases, by a tenfold increase). This was attributed to the grain boundary dislocation strain fields. The lattice distortion that occurs due to GB dislocations may vary significantly depending on the type of GB, whether planar or nonplanar, on the type of misorientation (in plane or out of plane), and of course on the misorientation angle. For example, a recent study showed that, at the same misorientation, [010]-tilt (valley type) and [100]-tilt (rooftop-like) grain boundaries form a less severe obstacle to current flow than [001]-tilt boundaries [40].

In this paper, we investigate the possible role of grain boundaries in controlling the strain dependence of J_c in coated conductors. The effect of strain on J_c of full-width coated conductors is compared to that of single grain boundaries (GBs) isolated from the same coated conductors using laser or focused ion beam (FIB) bridges across a few or individual grain boundaries. The lattice strain deduced from the strain dependence of J_c is then compared to that measured across [001]-tilt boundaries of PLD grown bicrystals.

2. Experimental details

2.1. Sample preparation

The coated conductors consist of a YBCO layer, nominally 0.8 μm thick, that is deposited onto a grain-aligned substrate by the *ex situ* metal–organic deposition route [41, 42]. This technique results in a laminar YBCO grain structure with meandering grain boundaries that lie in no particular plane, quite different from the case of YBCO grown by the *in situ* PLD method, where the GBs are planar and generally lie parallel to the c-axis of YBCO [43]. Grain alignment is introduced within a 75 μm thick textured NiW substrate, by means of the rolling-assisted biaxially-textured-substrate (RABiTS™) technique [44, 45]. Samples with MOD deposited YBCO on the textured substrates are designated MOD-RABiTS. Their self-field critical current density is around 3.0 MA cm^{-2} at 76 K.

Three 100 μm wide by 300 μm long bridges were cut in random positions by laser in the MOD-RABiTS tapes. The MOD-YBCO layer was chemically removed after the strain experiment was completed, and a grain orientation map of the exposed yttria-stabilized zirconium (YSZ) buffer layer was obtained with electron backscatter diffraction (EBSD). The a-axis orientation map of one of the bridges is shown in figure 1(a), while its grain boundary misorientation map is shown in figure 1(b). The 20–50 μm template grains of the NiW and its buffer overlayers are clearly visible in the bridge. A wide spread in grain misorientation in the general range of 3°–10° was measured in each bridge. The sample details are listed in table 1.

Two single grain boundary samples were cut with the FIB after the YBCO grain boundary misorientation from the same coated conductor was established. These bridges were 8 μm wide, as presented in figure 1(c). One sample had a 2.5° GB isolated with the FIB and one had a 4° GB.

The 200 nm thick YBCO thin films were deposited by pulsed-laser deposition on 4 mm × 12 mm single- and bicrystalline $SrTiO_3$ substrates. The bicrystalline substrates had [001]-tilt grain boundaries of 4°, 6°, 7.5° and 12°, respectively, that were oriented across the width of the substrate, and bridges either 200 or 500 μm wide were patterned on them. All samples were close to being optimally doped, with critical temperatures ranging from 90.5 to 90.9 K. Experimental parameters for YBCO film deposition were described in detail in previous studies [46, 47].

2.2. Measurement procedure

The dependence of J_c on axial strain was measured at 76 K with a 98 wt% Cu–2 wt% Be beam in a four-point bending apparatus. The samples were soldered onto the surface of the

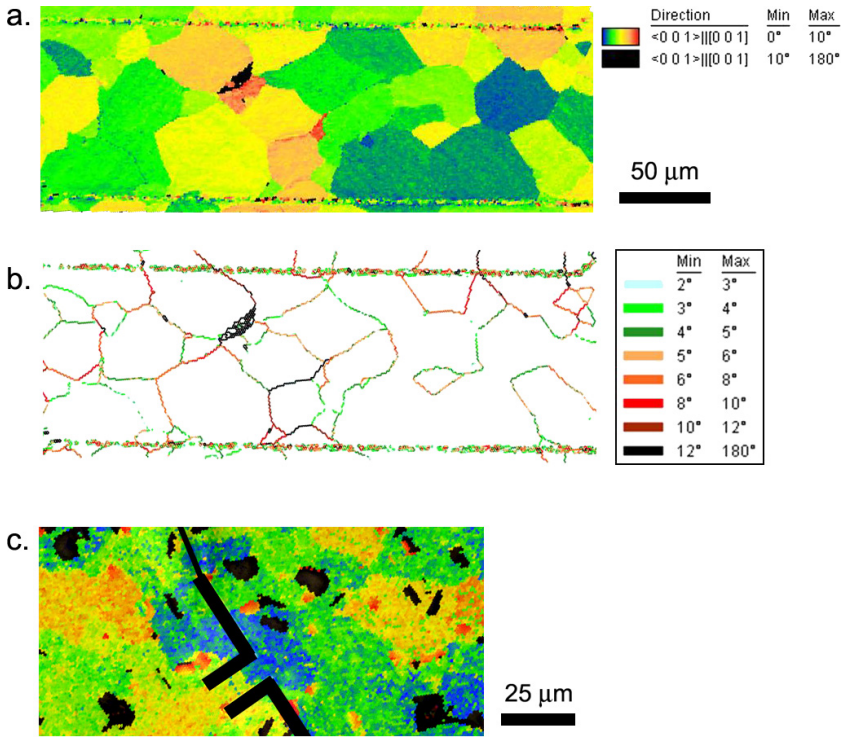

Figure 1. (a) *a*-axis orientation map of the YSZ layer in the 100 μm wide and 300 μm long laser-cut bridge-1. The laser tracks are the two horizontal lines in the figure where the grain orientation could not be determined. (b) Grain boundary misorientation map of the YSZ buffer layer in bridge-1. The current path is limited by grain boundaries of at least 6° misorientation that cover the entire width of the bridge. (c) *a*-axis orientation map of the YBCO layer in the isolated grain boundary FIB-2 with a 2.5° misoriented grain boundary. The FIB cuts are indicated by the black lines that have been drawn in the image. The bridge is 8 μm wide.

Table 1. Sample details and parameter values used in equation (1).

Sample number	Angle (deg)	Sample type	$J_c(0)$[a] (MA cm^{-2})	$J_c(\varepsilon_m)$[b] (MA cm^{-2})	ε_m (%)	a (−)
MOD-1	—	Full-size MOD-RABiTS	3.14	3.14	0.05	8 700
Bridge-1	—	100 μm MOD-RABiTS	1.04	1.04	−0.07	6 900
Bridge-2	—	100 μm MOD-RABiTS	0.86	0.86	0.05	7 350
Bridge-3	—	100 μm MOD-RABiTS	1.65	1.65	0.15	5 640
FIB-1	4	MOD grain boundary	4.62	4.63	−0.05	10 500
FIB-2	2.5	MOD grain boundary	4.40	4.43	−0.15	10 500
SC-1	0	Single-crystalline STO	3.95	3.96	−0.13	7 613
SC-2	0	Single-crystalline STO	4.25	4.26	−0.11	7 613
GB4°	4	Bicrystalline STO	1.34	1.93	−0.90	7 613
GB6°-1	6	Bicrystalline STO	0.72	1.17	−0.96	7 613
GB6°-2	6	Bicrystalline STO	1.10	1.47	−0.87	7 613
GB7.5°-1	7.5	Bicrystalline STO	0.45	0.53	−0.65	7 613
GB7.5°-2	7.5	Bicrystalline STO	0.28	0.38	−0.85	7 613
GB12°	12	Bicrystalline STO	0.08	0.09	−0.43	7 613

[a] J_c at zero applied strain.
[b] Maximum J_c at applied strain ε_m when the applied strain cancels the initial strain state of the YBCO.

beam by use of 97 wt% In–3 wt% Ag solder with a melting temperature of 143 °C. Axial strain was applied by bending the beam, with either the sample on top (axial compressive strain), or on the bottom (axial tensile strain) of the beam. The transport critical current was determined with an electric field criterion of 1 μV cm^{-1} and an uncertainty of about 0.5%. Strain was measured directly with strain gages mounted on both sides of the beam. The coated conductors with the FIB-isolated grain boundaries were oriented on the bending beam in such a way that the strain was applied along the length of the bridge, perpendicular to the grain boundary.

Strain was applied to the YBCO-STO films by gluing the substrates in a 4 mm × 12 mm slot that was machined in the CuBe bending beam (see figure 2). Only axial compressive strain was applied to these films, because the substrates break at a tensile strain of less than 0.05% although, in some cases, they can withstand axial compressive strains of over −0.8%. The transport critical current of the thin films at each level

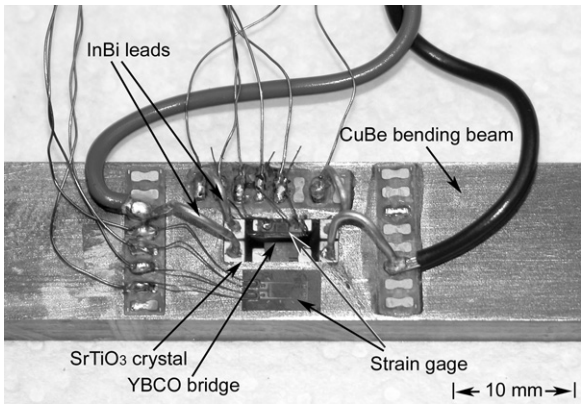

Figure 2. A single-crystalline STO substrate with a YBCO thin film is embedded in a slot machined in the CuBe bending beam. The applied strain is measured with a strain gage on the bending beam and, in some cases, with a strain gage mounted directly on the crystal. The leads for the 4-point measurement are made from low-temperature InBi solder wires.

of strain was determined within 1% uncertainty by use of an electric field criterion of 1 μV cm^{-1} in the case of single-crystalline films, or a voltage criterion of 1 μV in the case of bicrystalline films. To avoid sample heating, low-resistivity contacts capable of carrying in excess of 5 A, and flexible enough to withstand up to -0.8% compressive strain, were made by use of low melting temperature 63.3 wt% In–36.7 wt% Bi solder wires. The wires were soldered at 72 °C to the silver layers that were deposited locally on top of the YBCO films, as seen in figure 2.

3. Results and discussion

A relatively large ($\sim$30%) reversible change in J_c with strain was measured in full-width MOD-RABiTS coated conductors (figure 3(a)). The decrease in J_c is fully reversible under compressive strain. The irreversible strain limit is 0.74% under tension, and the critical current reaches a maximum at 0.05% strain for this particular conductor (MOD-1). For clarity, only data taken below the irreversible strain limit are shown in figure 3(a). The occurrence of the maximum in J_c at nonzero applied strain is due in part to the mismatch in thermal expansion coefficient of the YBCO layer and the other (mostly the NiW metallic) components of the conductor, and in part from strain arising from the difference in lattice parameters between the top buffer layer and the YBCO layer and possibly by grain boundary dislocations [39]. The strain dependence can be well described empirically with a power-law function [24]:

$$J_c(\varepsilon) = J_c(\varepsilon_m)(1 - a|\varepsilon - \varepsilon_m|^{2.18\pm0.02}). \quad (1)$$

Here $J_c(\varepsilon_m)$ is the maximum critical current density that is reached when the YBCO layer is at its minimum strain state at the applied strain ε_m. The constant a expresses the strain sensitivity of the sample. The parameter values used to describe the data are listed in table 1.

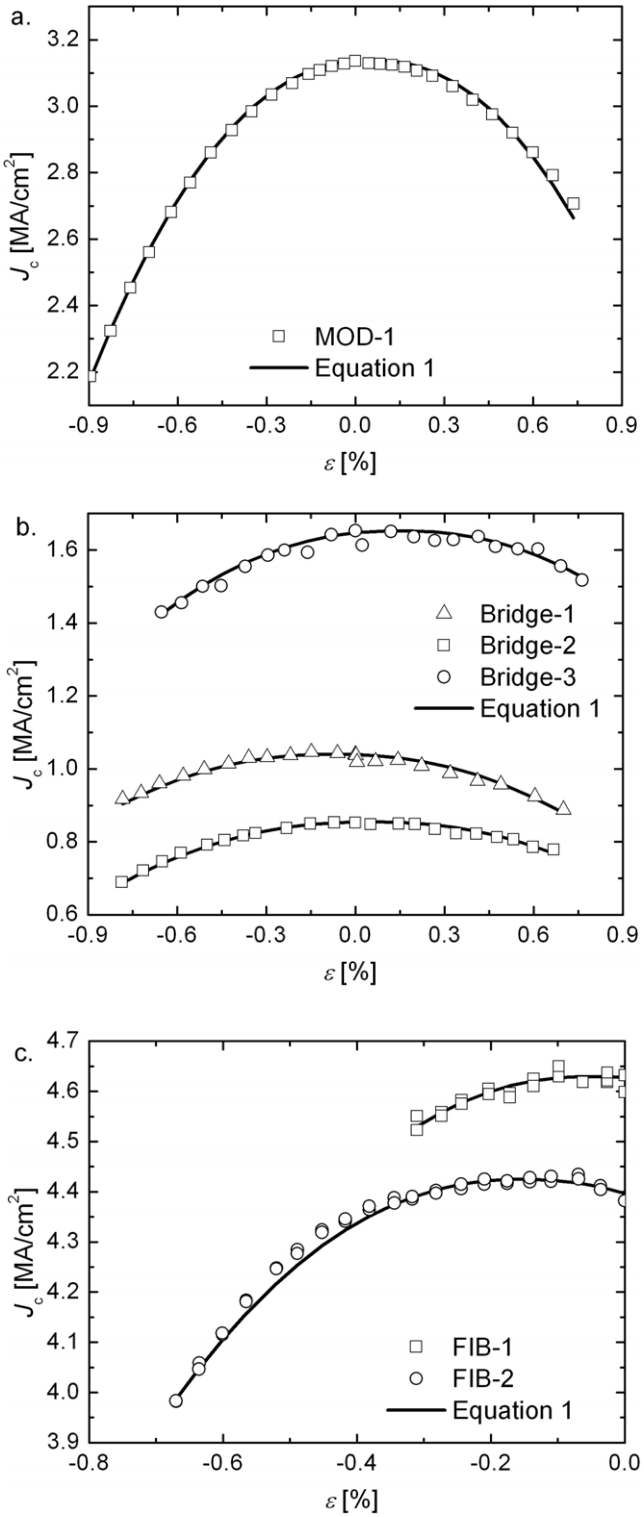

Figure 3. (a) The reversible change in J_c of full-width MOD-RABiTS coated conductor MOD-1 as a function of applied strain. (b) J_c as a function of strain of the three laser-cut bridges. (c) J_c as a function of strain of the two FIB-isolated grain boundaries. Only reversible data are shown for clarity. The solid lines in the figures fit the data with equation (1).

One of the main questions to be answered is whether the reversible strain dependence of J_c in YBCO coated conductors originates from within the grains, from the grain boundaries, or

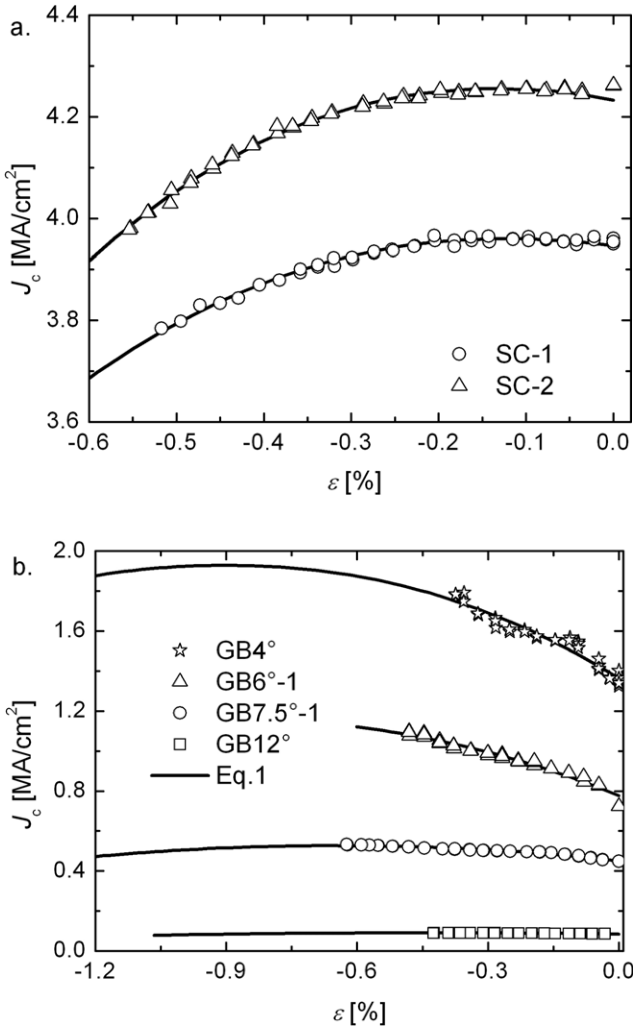

Figure 4. (a) Critical current density as a function of applied strain of two single crystal YBCO films deposited on STO substrates. (b) Critical current density as a function of applied strain of four YBCO films deposited on bicrystalline STO substrates with [001]-tilt grain boundaries. The solid lines are a fit to the data with equation (1).

from a combination of the two. A first approach to answering this question is to measure the J_c–strain dependence of well-defined grains and grain boundaries of YBCO. The critical current density of two single crystal YBCO films grown on STO substrates decreases with increasing compressive strain after a maximum in J_c is reached at -0.12% strain, as presented in figure 4(a). The films have initial J_c values of 3.95 and 4.25 MA cm^{-2}, which are reduced to 3.79 and 4.05 MA cm^{-2} at -0.5% strain. This change is not due to cracking of the film, but is fully reversible, as J_c fully recovers when the compressive strain is released. The effect of uniaxial compressive strain on J_c of four YBCO thin films with [001]-tilt grain boundaries is presented in figure 4(b). What is striking in this plot is that both the 4° and 6° GBs show a steep rise in J_c and the compressive strain is raised, but this effect is much smaller as the grain boundary misorientation increases. However, all data are well fitted by equation (1).

Although at first sight the strain dependence of J_c of the coated conductors, the single crystals, and the thin-film grain boundaries appears to be quite different, it has been recently shown that J_c follows the same functionality described by equation (1), as shown in [39]. Only the internal strain state of the YBCO after film deposition is different between the samples, and this difference results in a shift of the maximum in J_c as a function of applied strain, consequently, a different value of ε_m is generated in equation (1). The YBCO films deposited on single-crystalline STO substrates are under a tensile strain of about 0.1%–0.15%. However, large initial tensile strain values in GBs on STO are implied by figure 4(b), showing that the strain fields of the GB dislocations are exerting a considerable influence on the superconducting channels between the dislocations. The effective tensile strain deduced form equation (1) is around 0.9% for the 4° and 6° [001]-tilt grain boundaries and slightly lower for the 7° boundary. The 12° boundary is under only 0.43% tension, perhaps because the channels are now effectively closed and the strain at the GB becomes much more homogeneous along the GB length.

The first approach to measuring the strain dependence of grains in MOD-RABiTS was by laser-patterning 100 μm wide bridges into the coated conductors. The bridges are between 2 and 5 grains wide, which, as shown in figure 1(a), forces transport current to flow in part over higher-angle grain boundaries. All bridges contain grain boundaries that exceed 6°, as can be seen from the grain boundary orientation map in figure 1(b). The limited width of the current path also lowers J_c of the bridge by a factor of 1.5–3, compared to that of a full-size conductor; J_c of the bridges range from 0.85 to 1.65 MA cm^{-2}. The dependence of the critical current density on strain of the three bridges is shown in figure 3(b) for both applied compressive and applied tensile strain. The dependence of J_c on strain of the bridges is fully reversible and can also be described by equation (1), as is again shown by the solid lines in the figure. Besides the difference in J_c, the main difference between the bridges and the full-width coated conductor is the initial strain state of the YBCO layer, which defines the location of the peak in the J_c–ε curve (see table 1). The strain state of the YBCO layer in the bridges ranges from -0.07% compression to 0.15% tension ($=-\varepsilon_m$), whereas the YBCO in the full-width coated conductor is under -0.05% compression. We assume that this is due to differences in the GB properties, and also note that these values are much smaller than for the PLD grown GBs.

Some of the laser-patterned bridges were strained beyond the irreversible strain limit (results not shown). The damage was investigated by examining the damage in the YSZ buffer layer after the YBCO layer was chemically removed. The image presented in figure 5 clearly shows the grains of the YSZ layer that overlay the grains in the RABiTS substrate and the laser tracks that define the bridge. Large cracks that are following some of the grain boundaries in the YSZ layer, indicated by arrows, are visible as well. These cracks most likely developed at tensile strains that exceed the irreversible strain limit of the buffer and/or the YBCO layer, which resulted in the irreversible degradation of J_c. Apparently grain boundaries in the ceramic YSZ layer or even in the NiW substrate are mechanically weaker than the grains themselves,

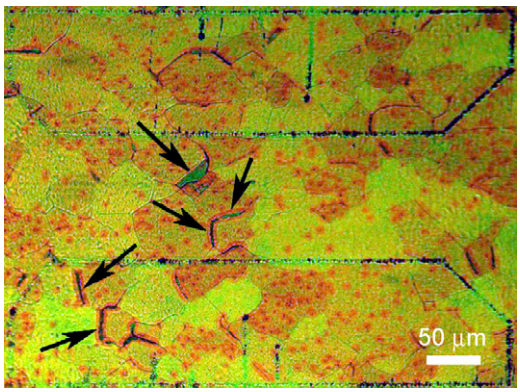

Figure 5. Optical image of the YSZ buffer layer of laser-patterned bridge-1 after J_c was measured as a function of strain into the irreversible range and after chemical removal of the YBCO layer. The 100 μm wide bridge formed by the laser tracks and the grain boundaries in the YSZ layer are clearly visible. The arrows indicate cracked grain boundaries.

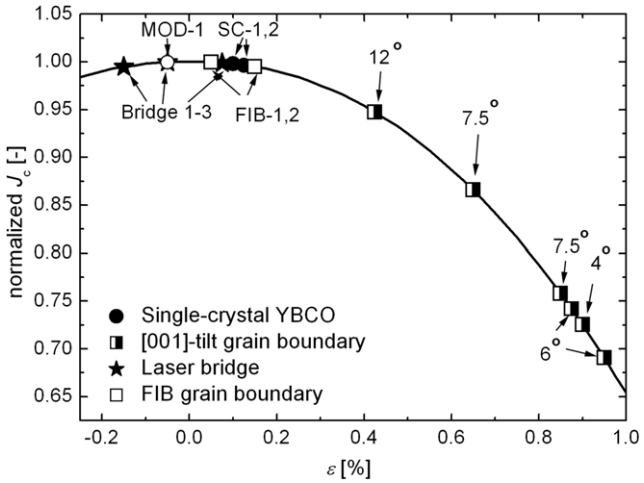

Figure 6. The initial strain state of the YBCO layer in all the samples investigated is plotted on the J_c–ε curve defined by equation (1) (with $\varepsilon_m = 0$ and $J_c(0) = 1$). It is particularly striking that the *in situ* grown PLD [001]-tilt grain boundaries have an internal tensile strain of up to 0.96%, whereas the *ex situ* MOD-YBCO on RABiTS template have a much lower internal strain, including the single grain boundaries.

since no cracks seem to have penetrated the grains. This result is very similar to earlier observations in Bi-2223 tapes, where cracks develop predominantly at grain boundaries in the ceramic filaments when strain exceeds ε_{irr} [48]. This behavior is opposite from the discontinuous yielding at high strain of the Hastelloy C-276 substrate in coated conductors that were prepared by the co-evaporation inclined-substrate deposition process [18].

To make a direct comparison to the single GB experiments on STO bicrystals, we needed to isolate single grain boundaries from the MOD coated conductor with the FIB. Included in figure 3(c) are the J_c versus strain curves of two such grain boundaries (2.5° and 4°). The bridges forced current across these individual grain boundaries by laser cutting the rest of the YBCO layer. The J_c of the two GBs show exactly the same functional dependence on strain as the laser-cut bridges that were 2–5 grains wide, but with higher J_c, since their misorientations of 2.5° and 4° were smaller than the many 6° or greater GBs in the wider bridges. However, the initial strain state of these FIB-cut MOD grain boundaries is only slightly different from laser-cut bridges and the full-width coated conductor.

The critical current density of the FIB-isolated grain boundaries is comparable to that of the thin YBCO films that were deposited on single-crystalline STO substrates, but much higher than that of the 4° [001]-tilt grain boundary samples. The deviation between J_c in the FIB-isolated 4° grain boundary and the 4° [001]-tilt grain boundary that was deposited on STO is a direct result of the much smaller initial strain state of the FIB-isolated grain boundary (0.15%), compared to that of the [001]-tilt grain boundary (0.90%). The much higher J_c of the 4° grain boundary at ε_m (see table 1) in the MOD-RABiTS conductor is also caused by the meandering nature of the grain boundaries in MOD films, where the GB current-carrying cross-section is much larger than the film thickness times the film width [49].

The fact that the strain dependence of J_c is similar between full-width coated conductors, 2–5 grain wide coated conductors with laser-patterned bridges, and coated conductors with FIB-isolated grain boundaries shows explicitly that grains and grain boundaries contribute to the reversible strain effect in a comparable manner. Even the initial strain state of the grain boundaries in MOD-RABiTS is comparable to that of full-size coated conductors, as is summarized in figure 6, where the initial strain states of all of the various samples of this paper are compared. The normalized critical current density as a function of strain according to equation (1) is plotted (with parameter ε_m equal to zero, and $J_c(\varepsilon_m)$ equal to 1). The symbols indicate a quite variable initial strain state of the YBCO (equal to $-\varepsilon_m$ in table 1) that we suggest results from a combination of the mismatch in thermal contraction, the lattice mismatch and the strain from GB dislocations. Note especially that the initial strain state of the MOD-YBCO samples, whether full-width MOD-RABiTS coated conductors, laser-patterned bridges, or FIB-isolated single grain boundaries, varies only from −0.15% to 0.15%. These values are much lower than the 0.43%–0.96% strain and were deduced from the planar [001]-tilt PLD grain boundaries with misorientations from 4° to 12°. The implication is clear: *ex situ* MOD coated conductors have much lower strain at their grain boundaries. As shown by Feldmann *et al* [43, 49], MOD grain boundaries are not planar, but meander through space without lying in any one plane and so cannot be composed of the simple alternating GB dislocation-channel structure that is well established for [001]-tilt grain boundaries in PLD bicrystals [5, 50].

4. Conclusions

The role of grains and grain boundaries in the reversible strain effect of MOD-RABiTS coated conductors has been investigated. We compared the dependence of J_c on strain

of full-width coated conductors, coated conductors with laser-patterned bridges, and FIB-isolated grain boundaries from coated conductors. The results clearly show that the J_c–ε dependence of both grains and grain boundaries can be described using the same power-law function. The strain at which the peak in the J_c–strain curve occurs is a direct measure for the initial strain state of the YBCO film. The internal lattice strain of PLD grown [001]-tilt grain boundaries is 5–10 times higher than that of YBCO grain boundaries in MOD-RABiTS coated conductors. We suggest that this difference is due to the existence of regular periodic GB dislocations in the planar PLD grain boundaries; however, they are absent or quite aperiodic in the meandered, nonplanar GBs that form in *ex situ* MOD films. Cracks develop at the grain boundaries of the YSZ buffer layer at high strains, which indicates that the grain boundaries of the RABiTS template are mechanically weaker than the grains. This behavior is opposite from the discontinuous yielding that has been observed by other groups in buffered Hastelloy substrates.

Acknowledgment

The work at NIST and at FSU was supported in part by the US Department of Energy, Office of Electricity Delivery and Energy Reliability.

References

[1] Selvamanickam V *et al* 2008 Progress in scale-up of 2G HTS wire at superpower *High Temperature Superconductivity Program Peer Review (Arlington, VA)*
[2] Selvamanickam V *et al* 2008 *Physica* C **468** 1504–9
[3] Malozemoff A P *et al* 2008 *Supercond. Sci. Technol.* **21** 034005
[4] Dimos D, Chaudhari P and Mannhart J 1990 *Phys. Rev.* B **41** 4038–49
[5] Chisholm M F and Pennycook S J 1991 *Nature* **351** 47–9
[6] Campbell A M 1989 *Physica* C **162** 273–4
[7] Dimos D, Chaudhari P, Mannhart J and LeGoues F K 1988 *Phys. Rev. Lett.* **61** 219–22
[8] Ivanov Z G *et al* 1991 *Appl. Phys. Lett.* **59** 3030–2
[9] Hilgenkamp H and Mannhart J 1998 *Appl. Phys. Lett.* **73** 265–7
[10] Heinig N F, Redwing R D, Nordman J E and Larbalestier D C 1999 *Phys. Rev.* B **60** 1409–17
[11] Chaudhari P, Dimos D and Mannhart J 1990 *Earlier and Recent Aspects of Superconductivity* ed J G Bednorz and K A Müller (Heidelberg: Springer) pp 201–7
[12] Hilgenkamp H and Mannhart J 2002 *Rev. Mod. Phys.* **74** 485–549
[13] Mannhart J and Hilgenkamp H 1997 *Supercond. Sci. Technol.* **10** 880–3
[14] Hilgenkamp H and Mannhart J 1998 Band-bending and d-wave symmetry at interfaces in high-T_c superconductors *Twente-HTS Workshop on Superconducting Electronics (Enschede)*
[15] Hilgenkamp H and Mannhart J 1996 *Phys. Rev.* B **53** 14586–93
[16] Ekin J W, Finnemore D K, Li Q, Tenbrink J and Carter W 1992 *Appl. Phys. Lett.* **61** 858–60
[17] ten Haken B, ten Kate H H J and ten Brink J 1995 *IEEE Trans. Appl. Supercond.* **5** 1298–301
[18] Sugano M, Osamura K, Prusseit W, Semerad R, Itoh K and Kiyoshi T 2005 *Supercond. Sci. Technol.* **18** S344–50
[19] ten Haken B, Beuink A and ten Kate H H J 1997 *IEEE Trans. Appl. Supercond.* **7** 2034–7
[20] Kovac P and Bukva P 2001 *Supercond. Sci. Technol.* **14** L8–11
[21] Garcia-Moreno F, Usoskin A, Freyhardt H C, Wiesmann J, Dzick J, Heinemann K and Hoffmann J 1997 *Appl. Supercond.* **158** 1093–6
[22] Cheggour N, Ekin J W, Clickner C C, Verebelyi D T, Thieme C L H, Feenstra R and Goyal A 2003 *Appl. Phys. Lett.* **83** 4223–5
[23] Sugano M, Osamura K, Prusseit W, Semerad R, Itoh K and Kiyoshi T 2005 *Supercond. Sci. Technol.* **18** 369
[24] van der Laan D C and Ekin J W 2007 *Appl. Phys. Lett.* **90** 052506
[25] Cheggour N, Ekin J W, Thieme C L H, Xie Y-Y, Selvamanickham V and Feenstra R 2005 *Supercond. Sci. Technol.* **18** S319
[26] Uglietti D, Seeber B, Abacherli V, Carter W L and Flukiger R 2006 *Supercond. Sci. Technol.* **19** 869–72
[27] Sugano M, Nakamura T, Manabe T, Shikimachi K, Hirano N and Nagaya S 2008 *Supercond. Sci. Technol.* **22** 115019
[28] Gao L *et al* 1994 *Phys. Rev.* B **50** 4260–3
[29] Pickett W E 1997 *Appl. Phys. Lett.* **78** 1960–2
[30] Chen X J, Lin H Q and Gong C D 2000 *Phys. Rev.* B **61** 9782–5
[31] Sato H, Tsukada A, Naito M and Matsuda A 2000 *Phys. Rev.* B **61** 12447–56
[32] Welp U *et al* 1992 *Phys. Rev. Lett.* **69** 2130–3
[33] Bud'ko S L, Guimpel J, Nakamura O, Maple M B and Schuller I K 1992 *Phys. Rev.* B **46** 1257–60
[34] Belenky G L *et al* 1991 *Phys. Rev.* B **44** 10117–20
[35] Locquet J-P *et al* 1998 *Nature* **394** 453–6
[36] Zhai H Y and Chu W K 2000 *Appl. Phys. Lett.* **76** 3469–71
[37] Kao H L, Kwo J, Fleming R M, Hong M and Mannaerts J P 1991 *Appl. Phys. Lett.* **59** 2748–50
[38] Si W and Xi X X 2001 *Appl. Phys. Lett.* **78** 240–2
[39] van der Laan D C, Haugan T J and Barnes P N 2009 *Phys. Rev. Lett.* **103** 027005
[40] Held R, Schneider C W, Mannhart J, Allard L F, More K L and Goyal A 2009 *Phys. Rev.* B **79** 014515
[41] Verebelyi D T *et al* 2003 *Supercond. Sci. Technol.* **16** L19
[42] Rupich M W, Verebelyi D T, Zhang W, Kodenkandath T and Li X P 2004 *MRS Bull.* **29** 572
[43] Feldmann D M, Holesinger T G, Cantoni C, Feenstra R, Nelson N A, Larbalestier D C, Verebelyi D T, Li X and Rupich M 2006 *J. Mater. Res.* **21** 923
[44] Goyal A *et al* 1996 *Appl. Phys. Lett.* **69** 1795
[45] Norton D P *et al* 1996 *Science* **274** 755
[46] Haugan T, Barnes P N, Wheeler R, Meisenkothen F and Sumption M 2004 *Nature* **430** 867–71
[47] Haugan T, Barnes P N, Brunke L, Maartense I and Murphy J 2003 *Physica* C **397** 47–57
[48] van der Laan D C, Ekin J W, van Eck H J N, Dhallé M, ten Haken B, Davidson M W and Schwartz J 2006 *Appl. Phys. Lett.* **88** 022511
[49] Feldmann D M, Holesinger T G, Feenstra R, Cantoni C, Zhang W, Rupich M, Li X, Durrel J H, Gurevich A and Larbalestier D C 2007 *J. Appl. Phys.* **102** 083912
[50] Song X, Daniels G, Feldmann D M, Gurevich A and Larbalestier D C 2005 *Nat. Mater.* **4** 470–5